

Compact UWB MIMO Antenna for 5G Millimeter-Wave Applications

Mohamed Atef Abbas^{1,2,*}, Abdelmegid Allam³, Abdelhamid Gaafar², Hadia M. Elhennawy¹ and Mohamed Fathy Abo Sree^{2,*}

¹ Department of Electronics and Communications Engineering, Ain Shams University, Cairo 11566, Egypt

² Department of Electronics and Communications Engineering, Arab Academy for Science, Technology and Maritime Transport, Cairo 11799, Egypt

³ Head of Information Technology, GUC, Cairo 101516, Egypt

* Correspondence: m.atef.abbas@aast.edu (M.A.A.); mohamed.fathy@aast.edu (M.F.A.S.)

Abstract: This paper presents a printed multiple-input multiple-output (MIMO) antenna with the advantages of compact size, good MIMO diversity performance and simple geometry for fifth-generation (5G) millimeter-wave (mm-Wave) applications. The antenna offers a novel Ultra-Wide Band (UWB) operation from 25 to 50 GHz, using a Defective Ground Structure (DGS) technology. Firstly, its compact size makes it suitable for integrating different telecommunication devices for various applications, with a prototype fabricated having a total size of 33 mm × 33 mm × 0.233 mm. Second, the mutual coupling between the individual elements severely impacts the diversity properties of the MIMO antenna system. An effective technique of orthogonally positioning the antenna elements to each other increased their isolation; thus, the MIMO system provides the best diversity performance. The performance of the proposed MIMO antenna was investigated in terms of S-parameters and MIMO diversity parameters to ensure its suitability for future 5G mm-Wave applications. Finally, the proposed work was verified by measurements and exhibited a good match between simulated and measured results. It achieves UWB, high isolation, low mutual coupling, and good MIMO diversity performance, making it a good candidate and seamlessly housed in 5G mm-Wave applications.



Citation: Abbas, M.A.; Allam, A.; Gaafar, A.; Elhennawy, H.M.; Sree, M.F.A. Compact UWB MIMO Antenna for 5G Millimeter-Wave Applications. *Sensors* **2023**, *23*, 2702. <https://doi.org/10.3390/s23052702>

Academic Editors: Antonio Lázaro, Christian Vollaie, Naser Ojaroudi Parchin, Chan Hwang See and Raed A. Abd-Alhameed

Received: 27 December 2022

Revised: 16 February 2023

Accepted: 23 February 2023

Published: 1 March 2023



Copyright: © 2023 by the authors. Licensee MDPI, Basel, Switzerland. This article is an open access article distributed under the terms and conditions of the Creative Commons Attribution (CC BY) license (<https://creativecommons.org/licenses/by/4.0/>).

Keywords: MIMO antenna; UWB; 5G; DGS; ECC; CCL; FDTD

1. Introduction

There is no doubt that this era is one of wireless communication technology that provides its contributed to the development of very high data rates, higher capacity, and reliability in communication applications used daily by a wide range of people [1,2]. Recently, Ultra-Wide Band (UWB) technology has been addressed in wireless communication systems due to its high data rates and low fabrication cost. Unfortunately, reflection and diffraction of an electromagnetic wave are the main obstacles in the dense medium, which cause multipath fading problems in UWB technology. Multiple-Input Multiple-Output (MIMO) technology has been proposed to alleviate multipath fading and increase transmission quality in wireless communication systems [3,4]. MIMO antenna systems associated with UWB technology provide an increase in the capacity linearly with the number of antennas without the need to add an additional frequency spectrum or increase the power resources. However, the design is affected by the mutual coupling between the antenna elements and the spatial correlation between them [5,6].

Concerning the separation between the antenna elements, the mutual coupling is inversely proportional to it. However, this distance should be chosen to be at a minimum between $\lambda/4$ and $\lambda/2$ to have a mutual coupling of less than -15 dB and therefore have an efficient working MIMO system. Additionally, a larger MIMO system size results from the increased separation between antenna units. As a result, while designing MIMO antennas,

trade-offs between the total size of MIMO systems and the minimizing of mutual coupling should be taken into account [7].

Many researchers aim to enhance the performance of different parameters such as bandwidth, compact size, gain, efficiency, mutual coupling and diversity properties in the Fifth Generation (5G) Millimeter-Wave (mm-Wave) antenna design. So, they use several enhancement techniques to obtain the best performance, like substrate choice, corrugation, multi-element, dielectric lens and mutual coupling reduction techniques [8,9]. First and foremost, the substrate used in antenna fabrication is critical. For antenna fabrication, various substrates with varying permittivity and loss tangents are available. As a result, a substrate with a lower relative permittivity and a lower loss tangent will increase gain while decreasing power loss [10]. Second, the corrugation structure, which removes the metal part of the radiator's edge, can help improve the bandwidth and front-to-back ratio [11]. In terms of the multi-element technique, it increases an antenna's gain while also increasing its bandwidth and efficiency. As a result, structures can meet requirements such as high gain and wide bandwidth that a single antenna cannot. Furthermore, the dielectric lens can transmit electrostatic radiation in only one direction, increasing an antenna's directivity and gain [12,13]. Dielectric lenses of various shapes are created using the same or different substrate material. Finally, mutual coupling reduction techniques mitigate the effect of multiple elements on antenna performance. This technique, also known as the isolation technique, is critical for achieving the best diversity performance from MIMO antennas.

A variety of approaches have been used to reduce mutual coupling between MIMO antenna elements. Neutralization techniques, simultaneous matching of orthogonal feeding or elements, pattern diversity, and significant polarisation are all included [11–13]. In addition, many methods have been employed in an attempt to reduce coupling, including Defective Ground Structures (DGS), Electromagnetic Band Gap (EBG) substrates, complementary split ring resonators (CSRR), metamaterials, and parasitic resonators [14–17]. These methods, however, call for a sizable amount of circuit board space. Etching the isolating slots between the antenna elements is a different strategy. Numerous slot configurations, such as an F-shaped stub, a T-shaped slot, an L-shaped slot, or a vertical slot, have been tested [18–21]. Although the mutual coupling between the radiating antennas is reduced by these slots, the overall gain remains unchanged. In a 4-element MIMO antenna, linear slots were inserted in between the radiating slots to lessen mutual coupling [22]. In [23], etching linear slots between the radiators of a 4-element MIMO antenna system reduced the mutual coupling by an amount of 20 dB. A 4-element MIMO antenna with four T-shaped radiating elements was proposed by M. Alibakhshikenari [24]. This small, wideband antenna had a maximum gain of 5 dBi and a minimum isolation of 15 dB. This resulted from stubs on the bottom ground and a shortened ground plane. It was suggested in [25] to use a 2-port textile MIMO antenna with two half-ring-shaped antenna elements. In order to obtain a minimum isolation of 15.5 dB, the ground plane is defective. Dual patched wideband MIMO antennas with an inverted pair of L-shaped stubs in the ground were another design [26]. In comparison to other proposed designs, the isolation was roughly 20 dB, and the highest gain was 5.32 dBi. The main drawbacks of this system are that it is more complex and has low gain.

On the other hand, Diversity properties of MIMO systems like envelope correlation coefficient (ECC), Channel capacity loss (CCL), Diversity Gain (DG), Multiplexing Efficiency (ME) and Total Active Reflection Coefficient (TARC) are strongly affected by the mutual coupling between antenna elements of MIMO system [27–30]. Therefore, it is evident that a MIMO antenna system should have more diversity parameters to be evaluated in addition to the antenna's parameters. These metrics are not required for single-antenna elements but are required for multi-antenna devices.

Although significant work and research were made in the last half-decade to introduce reliable MIMO antennas with acceptable diversity parameters, In this work, the DGS and antenna element orientation are developed to achieve acceptable isolation along the operating band. In this study, a 4-port MIMO antenna system covering the frequency range

of 25 to 50 GHz is developed, constructed, and tested. The ground plane's carved slots between the antenna elements and the orthogonal orientation of the antenna elements form the design's foundation. A DGS is then used to deploy for mutual coupling reduction and gain enhancement after a reference antenna is tuned for bandwidth enhancement. The work is organised as follows; Section 2 presents the antenna design and optimization of a single antenna. Section 3, which is concerned with simulation and measurable outcomes, presents a brief summary of the theoretical basis, including diversity parameters. Section 5 serves as the paper's conclusion.

2. Antenna Design

Since the antenna is the pivot element of MIMO antenna systems, many researchers present different antennas adapted for this technology. Concerning mm-Wave applications, printed antennas are the best candidates for this technology because of their low cost, low profile, compact size, and good choice to achieve a functional element with a proper balance of performance and manufacturing complexity for millimeter wave applications.

Figure 1 depicts the suggested four-element MIMO antenna design taken into consideration in this study. In (a), the top view is shown, while (b) shows the bottom perspective (b). The constructed model of the antenna structure is shown in Figure 2. The modelling and simulation of this design are done using the Finite-Difference Time-Domain (FDTD) (CST Microwave Studio). The choice of the substrate material, RO4003C, for electronic circuit boards that provide high-frequency performance and low-cost circuit manufacturing was made since it is one of the most widely used industry-wide standard substrate material formats [31,32]. Figure 3 illustrates the measurement setup of the constructed antenna using the ROHDE & SCHWARZ ZVA67 Vector Network Analyzer [33]. The dimensions of the MIMO are $33 \times 33 \times 0.203 \text{ mm}^3$.

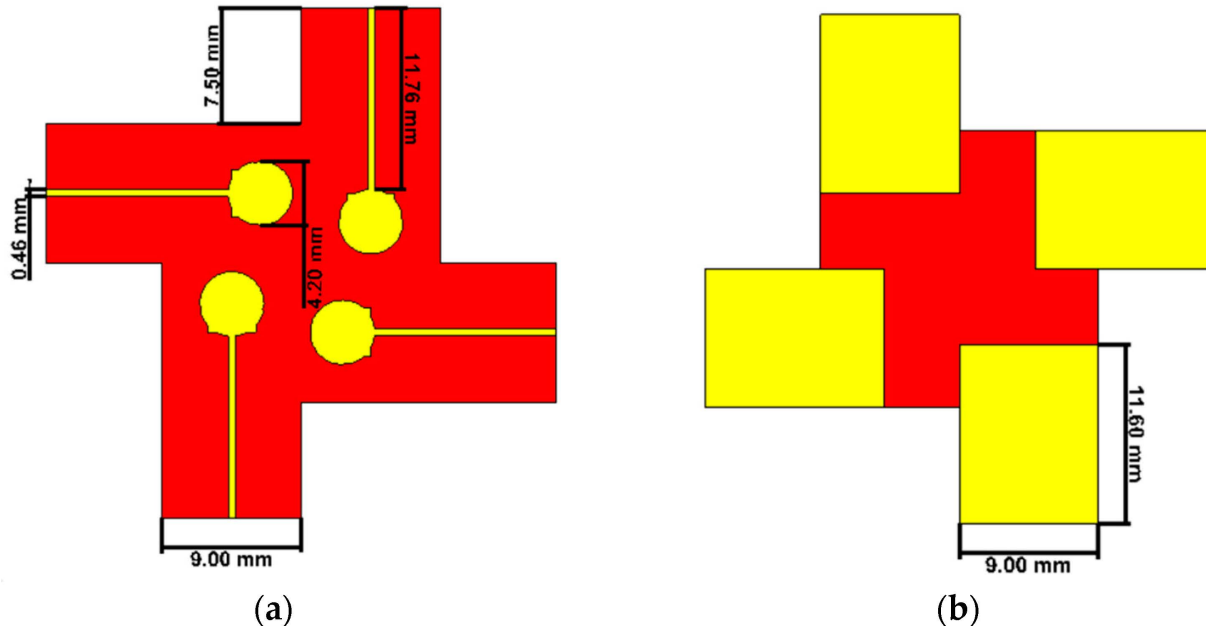


Figure 1. The proposed antenna (a) Top view. (b) Bottom view.

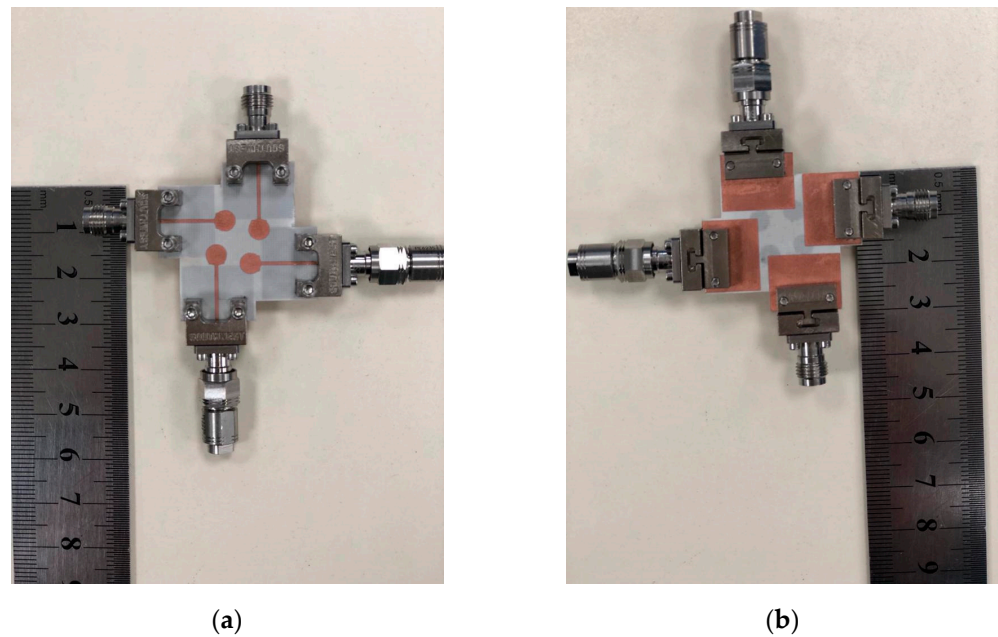


Figure 2. The fabricated prototype of 4 elements MIMO antenna (a) Top View (b) Bottom view.

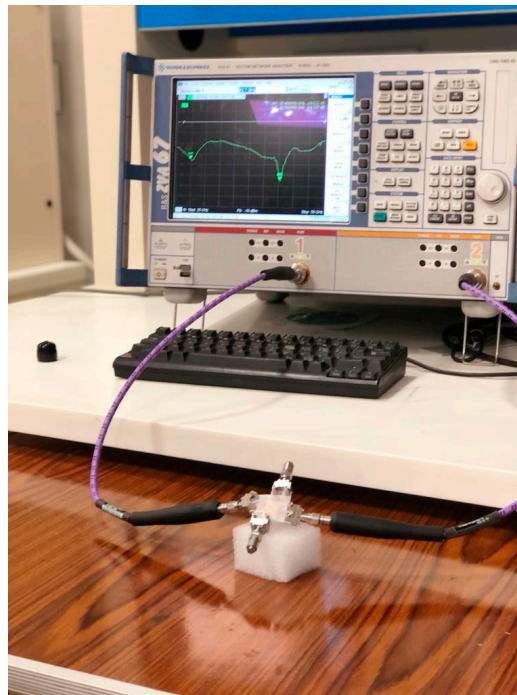


Figure 3. Measurement setup of proposed MIMO using ROHDE & SCHWARZ ZVA67 Vector Network Analyzer.

An overview of the sequential design evolution is shown in Figure 4. Figure 4 shows how the modelling begins with a single antenna element (a). as an initial step. Using well-known mathematical formulas, a rectangular patch antenna with inset feed and the full ground plane is produced it resonates at 30 GHz. The preliminary values of length L and width W can be determined from [34]:

$$W = \frac{c}{2f_r} \sqrt{\frac{2}{\epsilon_r + 1}} \quad (1)$$

$$L = L_{eff} - 2\Delta L \quad (2)$$

$$\Delta L = 0.412h \frac{(\epsilon_{reff} + 0.3) \left(\frac{W}{h} + 0.264\right)}{(\epsilon_{reff} - 0.258) \left(\frac{W}{h} + 0.8\right)} \quad (3)$$

$$\epsilon_{reff} = \frac{\epsilon_r + 1}{2} + \frac{\epsilon_r - 1}{2} \left(1 + 12 \frac{h}{W}\right)^{-0.5}, \quad \frac{W}{h} > 1 \quad (4)$$

$$L_{eff} = \frac{c}{2f_r \sqrt{\epsilon_{reff}}} \quad (5)$$

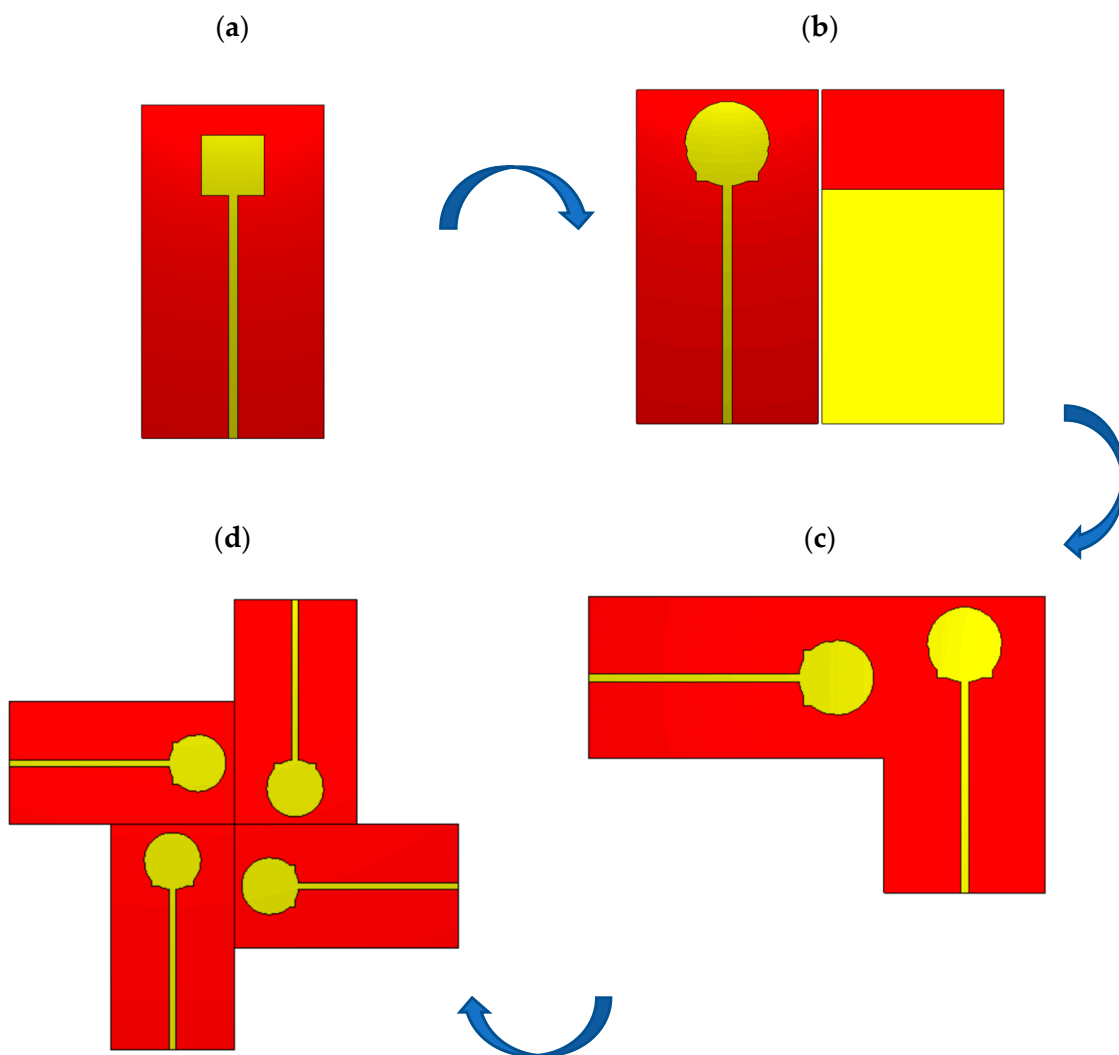


Figure 4. Steps of design (a) rectangular patch antenna with inset feed and full ground (b) single proposed antenna (top and bottom) (c) 2-port MIMO antenna with orthogonal orientation (d) Final step for 4-port MIMO antenna.

The rectangular patch antenna is improved for a larger band in the second step by etching the ground (DGS) and adding vertically and horizontally oriented circular slots to the three sides, as shown in Figure 4b. To reduce the mutual coupling, the MIMO structure is created for two ports utilizing an orthogonal orientation, as shown in Figure 4c. Based on this setup, Figure 4d shows a MIMO antenna structure with four ports to span the frequency range of 25 to 50 GHz.

The long microstrip feed in Figure 4b is a typical choice for measurements in the millimetric band. To accommodate the special connector needed for the antenna element,

additional length and width would need to be added to the grounded substrate. Figure 5 demonstrates the fixation of the connector of each individual antenna element. In addition, a separation between the fixation nuts of the connector and the radiator of MIMO antenna should attain a long length to separate them as shaded by black color.

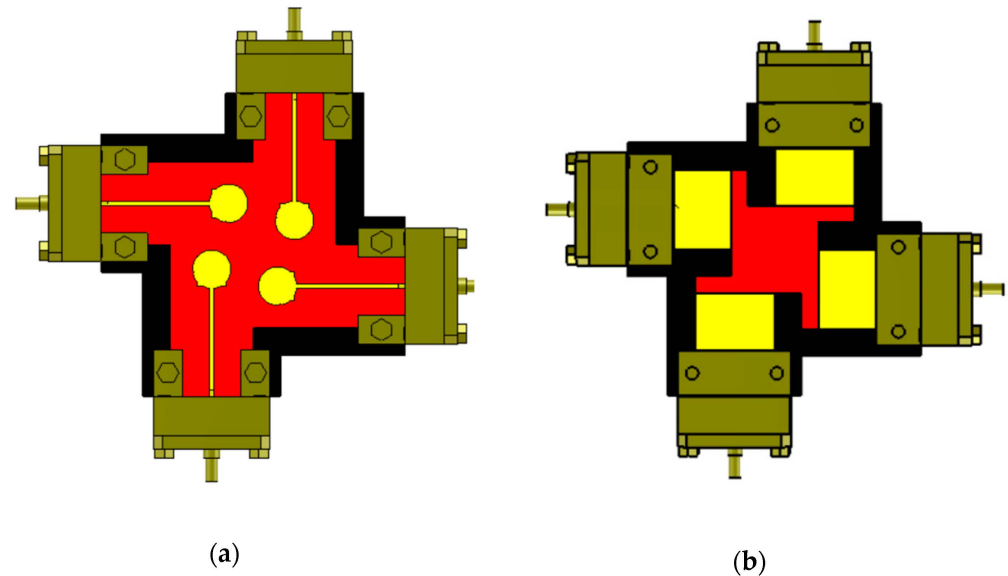


Figure 5. The prototype of 4 elements MIMO antenna with connector: (a) Top View (b) Bottom view.

The fabrication process includes many steps. Based on the available dielectric substrate, we select the appropriate one suitable for the required frequency band. The antenna is modelled on CST microwave studio simulator. The optimization process is developed. Then, the Gerber file and “.Sab” file are exported to the manufacturer. At this step the duty of the academic researchers is finished. On the fabrication side the mask of design is developed. The copper is etched from the top and bottom surfaces using chemical process.

3. MIMO Antenna Parameters for Performance Evaluations

When presenting a MIMO antenna along with other fundamental characteristics, Diversity parameters analysis is a must in addition to the fundamental antenna performance evaluations and parameters, such as bandwidth, resonance frequency, radiation patterns, gain, and efficiency. These characteristics are necessary for multi-antenna devices but not for single-antenna elements. The parameters used for this include the TARC, CCL, DG, and ECC. The next subsections go over these variables in relation to the suggested antenna design.

The antenna is fabricated as shown in Figure 3 and measured using ROHDE & SCHWARZ ZVA67 vector Network Analyzer. A demonstration of the S-parameters coefficients values can be seen in Figure 6. It is clear that the reflection coefficient level is below -10 dB over the whole band from 25 to 50 GHz, as shown in Figure 6a. The difference between measurement and simulated results is noticeable in the higher frequency band due to the connectors in the millimetric band and in the other environments. The measurement setup is not in a completely shielded room. On the other hand, the coupling parameters are below -20 dB on average. It reaches -40 dB to -50 dB in individual sub-bands, as shown in Figure 6b.

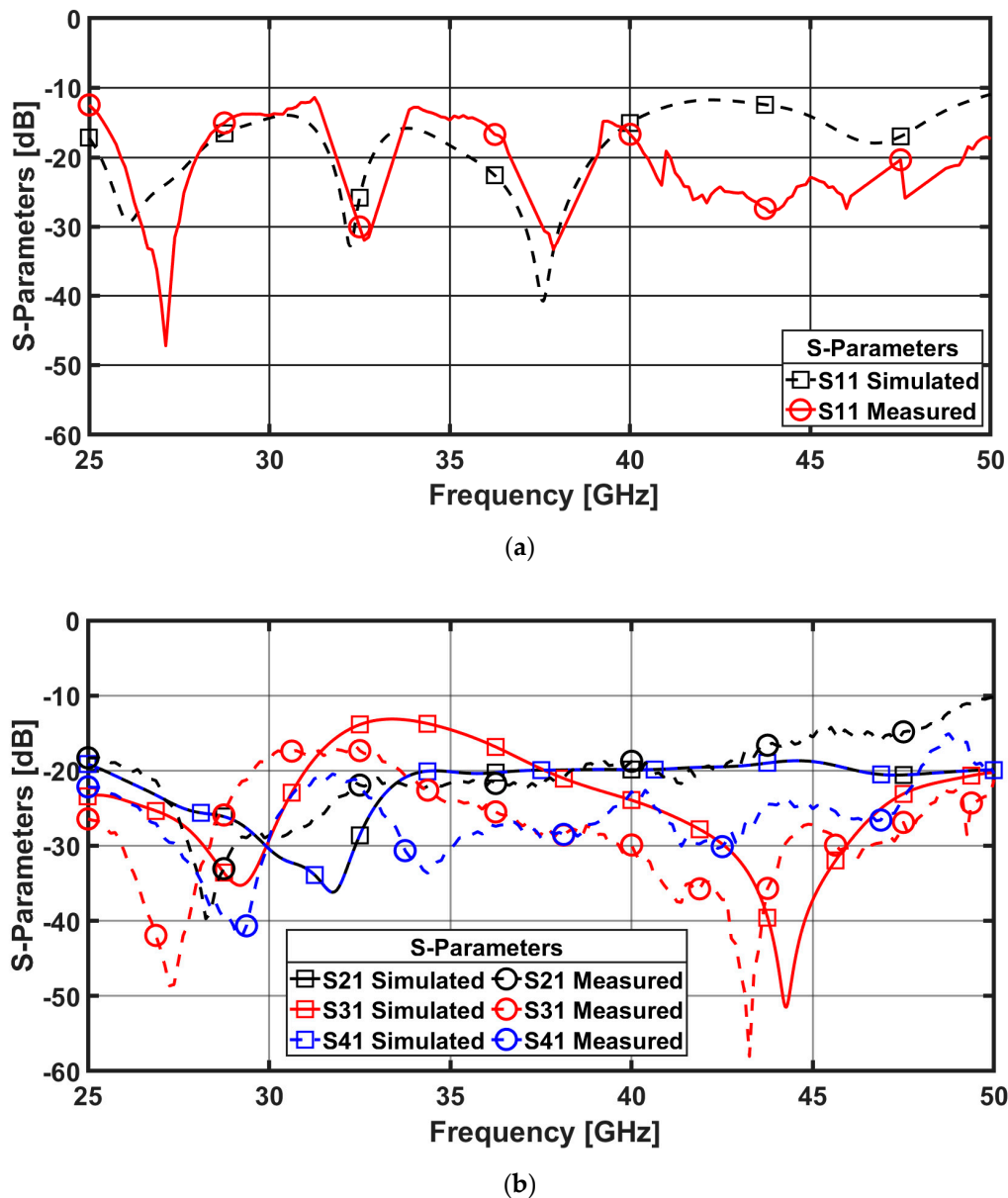


Figure 6. S-parameters coefficient (a) Reflection coefficient (b) Transmission coefficient.

3.1. Envelope Correlation Coefficient (ECC)

The level of correlation between various antenna components in a MIMO configuration is measured by ECC. Lower ECC results in less interdependence between the components and, as a result, better MIMO diversity performance. Equations (6) and (7), respectively, show how to compute the ECC from both the far field radiation pattern and the scattering parameters [28,35].

$$ECC = \rho_e = |\rho_{ij}| = \frac{|\int \int 4\pi [F_i(\theta, \phi)] \bullet [F_j(\theta, \phi)] d\Omega|^2}{\int \int 4\pi |F_i(\theta, \phi)|^2 d\Omega \int \int 4\pi |F_j(\theta, \phi)|^2 d\Omega} \quad (6)$$

where $i, j = 1, 2, 3, 4$, ρ_{ij} is the ECC between i^{th} and j^{th} antenna elements, while $F_i(\theta, \varphi)$ is the 3D radiation pattern field with excitation at port “ i ” and “•” denotes the Hermitian product and “ Ω ” is the solid angle.

$$ECC = \rho_e = |\rho_{ij}| = \frac{|S_{ii}^* S_{ij} + S_{ji}^* S_{jj}|^2}{(1 - (|S_{ii}|^2 + |S_{ji}|^2))(1 - (|S_{jj}|^2 + |S_{ij}|^2))} \tag{7}$$

where “*” is the complex conjugate of the S-parameter. When assessing any lossy antenna, it is crucial to note that obtaining the ECC values using S-parameters is inaccurate and significantly underestimates its values. Therefore, because they are more accurate, the results acquired from far-field radiation patterns are more useful [36]. However, this process is complex and requires advanced calculations. If the ECC is lower than 0.5, then it is within the acceptable limit and the MIMO diversity is considered good as shown in Figure 7. Which indicates that no correlation between elements.

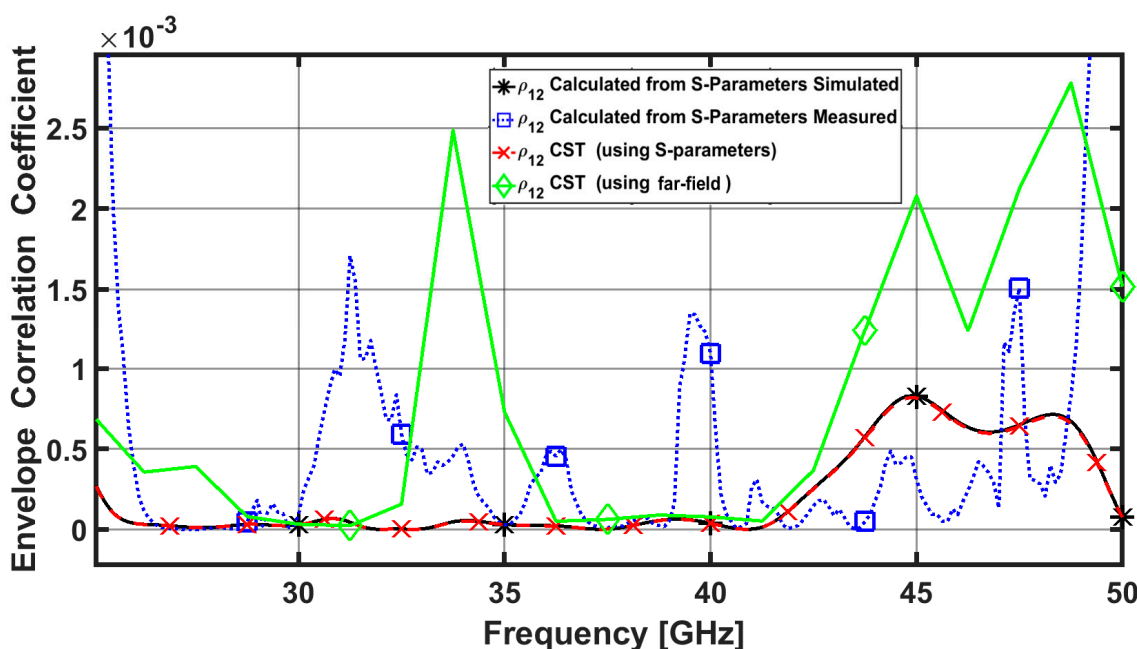


Figure 7. ECC of the proposed four-element MIMO antenna between port 1 and 2.

3.2. Diversity Gain (DG)

DG value is obtained from ECC, and it can be easily calculated using the following equation:

$$DG = 10 * \sqrt{1 - \rho_{ECC}} \tag{8}$$

It is clear that ECC and DG are inversely proportional to one another. A high DG value therefore indicates superior performance. The DG may be determined using both the far field radiation pattern and the scattering parameters, much like the ECC can [27]. Better isolation between the patch elements of the MIMO antenna is correlated with higher diversity gain values. More than 9.95 dB should be present in the DG. The estimated calculated values of the DG are higher than 9.99 dB across the antenna’s operating band, as shown in Figure 8. Which indicates the good diversity performance of the proposed MIMO antenna system.

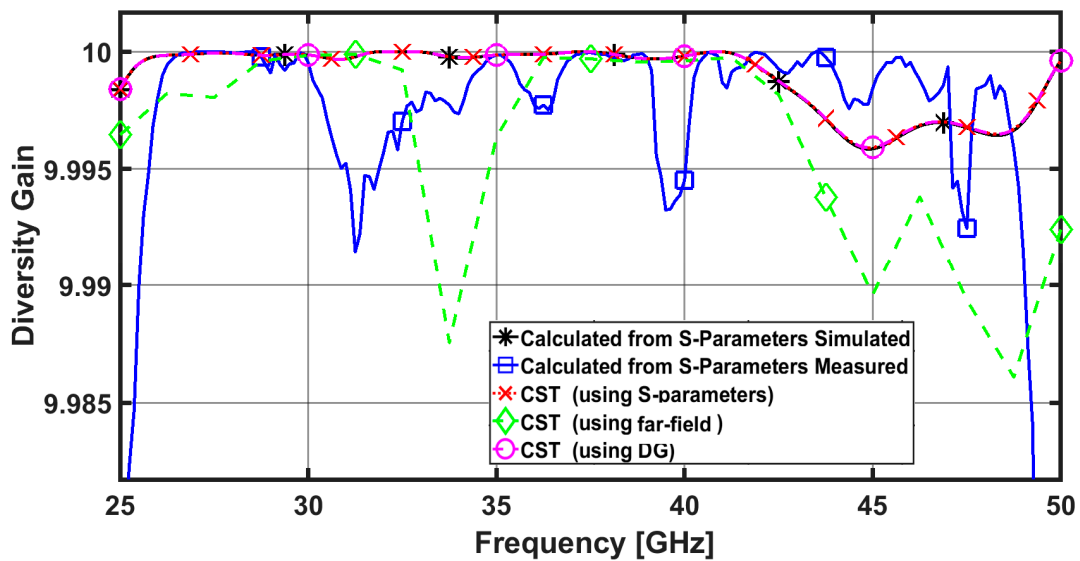


Figure 8. DG between ports 1 and 2 for the proposed four-element MIMO antenna.

3.3. Channel Capacity Loss (CCL)

The CCL parameter, which specifies the highest achievable limit of the information transmission rate, can be used to describe the channel capacity of MIMO systems. It calculates the ideal information transfer rate, in other words. An Equations from [37] can be used to derive the CCL parameter.

$$C(\text{Loss}) = -\log_2 \det(\psi^R) \quad (9)$$

where ψ^R indicates the correlation matrix at the receiving antenna.

$$\psi^R = \begin{bmatrix} \rho_{11} & \rho_{12} \\ \rho_{21} & \rho_{22} \end{bmatrix} \quad (10)$$

$$\rho_{ii} = 1 - (|S_{ii}|^2 + |S_{ij}|^2), \text{ for } i, j = 1 \text{ or } 2 \quad (11)$$

$$\rho_{ij} = -(S_{ii}^* S_{ij} + S_{ji}^* S_{ij}), \text{ for } i, j = 1 \text{ or } 2 \quad (12)$$

Figure 9 depicts the calculated and measured CCL. The CCL value is clearly less than 0.3 bps/Hz across the entire band. So, using the available CCL, it is possible to confirm that the proposed antenna provides a higher transmission data rate in any scattering environment.

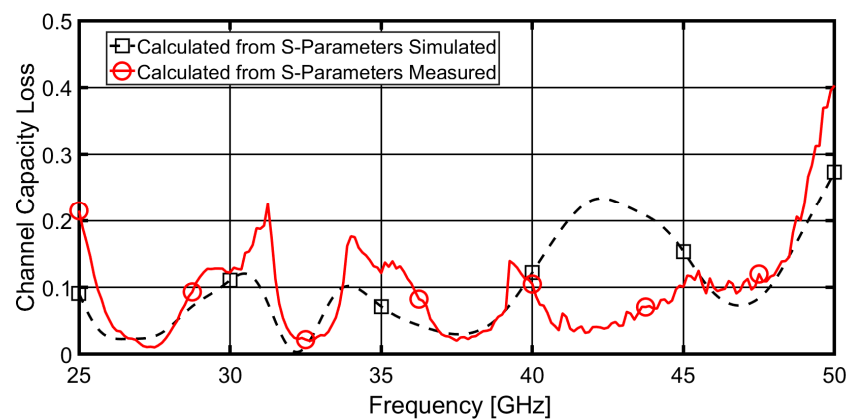


Figure 9. CCL of the proposed four-element MIMO antenna between port 1 and 2.

3.4. Multiplexing Efficiency (ME)

ME is defined as the ratio between the power of the real antenna and that of the ideal one. The maximum ME has been calculated as [38]:

$$\eta_{max} = \sqrt{\eta_i \eta_j (1 - |\rho_{eij}|^2)} \quad (13)$$

where η_i and η_j is the total efficiency of the i^{th} and j^{th} antenna elements and ρ_{eij} is the magnitude of complex correlation coefficients between i^{th} and j^{th} antenna elements. The simulated and the measured ME are around -1 dB within the band from 25 GHz to 50 GHz, as illustrated in Figure 10. Which indicate that the MIMO antenna system are considered as ideal from 80% to 92% all over the band.

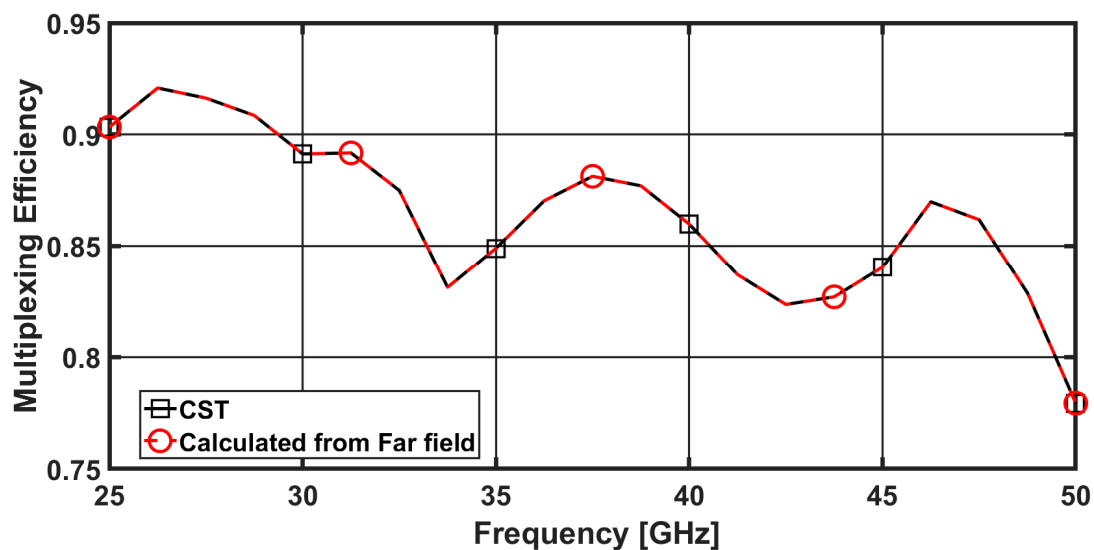


Figure 10. ME of the proposed four-element MIMO antenna between port 1 and 2.

3.5. Total Active Reflection Coefficient (TARC)

The ratio between the square roots of the total power reflected and the total power incident, is known as the total active reflection coefficient (TARC). It may be estimated using the S-parameters and depicts the random signal combinations and mutual couplings between the ports. TARC is the sole MIMO parameter that takes into account the unpredictable phases of incoming signals, which can have a significant impact on MIMO array behavior in certain circumstances. TARC of 4-port MIMO antenna can be calculated as [39,40]:

$$TARC = N^{-0.5} * \sqrt{\sum_{i=1}^N \left| \sum_{k=1}^N S_{ik} e^{j\theta_{k-1}} \right|^2} \quad (14)$$

where S_{ik} is the scattering parameter between the i^{th} and k^{th} ports, and θ_{k-1} is the excitation phase difference between the i^{th} and k^{th} ports.

The value of TARC for a MIMO communication system shouldn't exceed 0 dB. Figure 11 displays the measured and simulated values of TARC. The value of the proposed antenna's simulated and measured TARC is clearly under 10 dB for nearly the whole frequency range between 25 and 50 GHz where it is near to the reflection coefficients (the reference band), as can be seen from the Figure. The fabrication tolerance, test connectors, and connecting cables, as well as the surrounding test environment may all contribute to a slight difference between the measured and simulation findings.

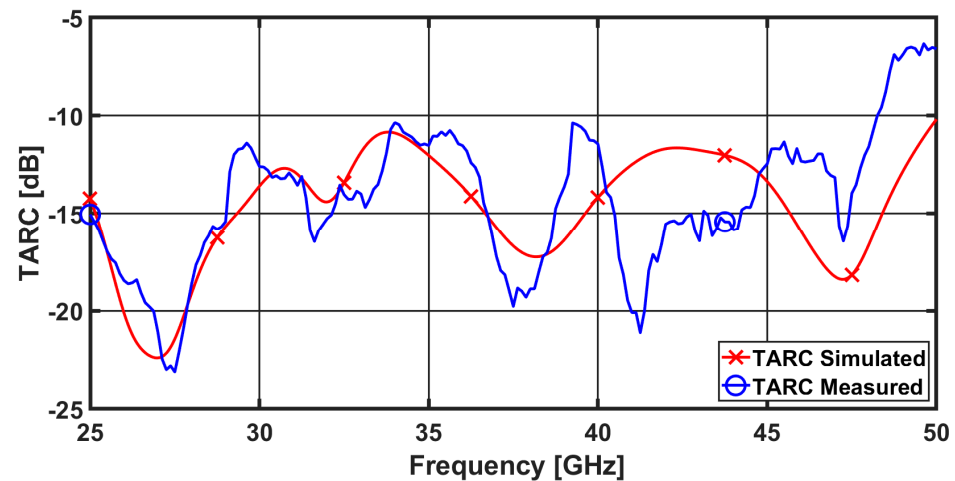


Figure 11. TARC simulated and measured results of the proposed four-element MIMO antenna.

4. Performance Comparison

In Table 1, a comparison between the proposed MIMO antenna system and the most recent MIMO work working in the 25–50 GHz region is made. The analysis takes several MIMO antenna characteristics into account. The proposed antenna with the same number of ports is more compact than [41–43]. In terms of realized gain, radiation efficiency, and isolation between antenna elements, it delivers superior MIMO performance than other small designs in [44–46]. Additionally, it has a high fractional bandwidth and a decreased mutual coupling. Its size is not the smallest, but compared to other literature work, it exhibits a considerable improvement in high isolation and superior MIMO diversity performance. This makes it possible to use the suggested antenna for 5G mm-wave applications. It's also crucial to note that the proposed design is straightforward and has symmetric geometry, making it simple to include into larger MIMO antennas with more radiating elements.

Table 1. Comparisons between the proposed MIMO antenna system and the published literature operating in 25–50 GHz band.

Reference	Physical Dimension (mm ²), Number of Ports	Substrate ϵ_r Thickness	Frequency, Band (B.W), Fractional B.W (GHz%)	MIMO Parameters					Mutual Coupling Reduction Technique
				ECC	DG	CCL	ME	TARC	
[41]	80 × 80 4 ports	Roger 5880, $\epsilon_r = 2.2$ 0.508	23–40, 17, 53%	<0.0014	NA	NA	NA	NA	DGS
[42]	23.75 × 42.5 4 Ports	Roger 5880, $\epsilon_r = 2.2$ 0.508	24–28, 4, 14.2%	<0.002	9.9	<0.001	N/A	N/A	DGS
[43]	45 × 45 4 Ports	FR-4 $\epsilon_r = 4.2$, 1.6	4.98–5.98, 1, 16.7%	<0.0022	9.95	<0.4	N/A	CALC.	Floating Parasitic Element
[44]	30 × 30 4 ports	Roger 5880, $\epsilon_r = 2.2$ 1.575	25–31, 6, 21.1%	<0.0005	NA	0.15	NA	NA	DGS
[45]	17 × 17 4 Ports	FR-4 $\epsilon_r = 4.2$, 0.8	3.4–3.6, 0.2, 5.5%	0.2	NA	57	CALC.	NA	Orthogonal Polarization
[46]	5 × 4 Single	Roger 5880, $\epsilon_r = 2.2$ 1.575	5.5–9.5, 4, 40%	N/A	N/A	N/A	N/A	N/A	N/A
Proposed Antenna	33 × 33 4 Ports	RO4003C, $\epsilon_r = 3.55$ 0.203	25–50, 25, 66%	<0.005	≈10	<0.25	>0.85	<−10	Orientation and DGS

5. Conclusions

The proposed MIMO antenna system has been designed to provide high isolation and UWB capability, with a perfect alignment orientation between the four elements and etching the ground using DGS. The proposed antenna system has achieved excellent performance parameters, such as low mutual coupling of less than -10 dB, low ECC of less than 0.005, low CCL of 0.25 bits/s/Hz, high DG of 9.999 dBi and low TARC of less than -10 dB, which shows a superior diversity performance. In addition, the wide operational bandwidth of 25 GHz, from 25 to 50 GHz, enables the antenna to be used in multiple applications. The compact design and low-cost design features make it suitable for mm-wave 5G applications and can be easily integrated into telecommunication devices. Furthermore, the suggested MIMO antenna system offers great performance and portability, making it an ideal choice for a wide range of 5G mm-wave applications.

Author Contributions: Conceptualization, A.A. and M.A.A.; methodology, A.A.; software, M.F.A.S. and M.A.A.; validation, M.F.A.S. and M.A.A.; writing—original draft preparation, M.A.A.; writing—review and editing, A.A., M.F.A.S. and M.A.A.; supervision, A.A., A.G. and H.M.E.; All authors have read and agreed to the published version of the manuscript.

Funding: This research received no external funding.

Institutional Review Board Statement: Not applicable.

Informed Consent Statement: Not applicable.

Data Availability Statement: Not all data is applicable. However, the MATLAB portion of the data is useful and can be shared. To access this data, please reach out to the first author via email.

Conflicts of Interest: The authors declare no conflict of interest.

References

1. Rappaport, T.S.; Sun, S.; Mayzus, R.; Zhao, H.; Azar, Y.; Wang, K.; Wong, G.N.; Schulz, J.K.; Samimi, M.; Gutierrez, F. Millimeter Wave Mobile Communications for 5G Cellular: It Will Work! *IEEE Access* **2013**, *1*, 335–349. [[CrossRef](#)]
2. Hasan, M.; Faruque, M.R.I.; Islam, M.T. Dual Band Metamaterial Antenna For LTE/Bluetooth/WiMAX System. *Sci. Rep.* **2018**, *8*, 1240. [[CrossRef](#)]
3. Katalinic, A.; Nagy, R.; Zentner, R. Benefits of MIMO Systems in Practice: Increased Capacity, Reliability and Spectrum Efficiency. In Proceedings of the Proceedings ELMAR 2006, Zadar, Croatia, 7–10 June 2006; pp. 263–266. [[CrossRef](#)]
4. Molisch, A.; Win, M. MIMO systems with antenna selection. *IEEE Microw. Mag.* **2004**, *5*, 46–56. [[CrossRef](#)]
5. Paulraj, A.; Gore, D.; Nabar, R.; Bolcskei, H. An Overview of MIMO Communications—A Key to Gigabit Wireless. *Proc. IEEE* **2004**, *92*, 198–218. [[CrossRef](#)]
6. Pi, Z.; Khan, F. An introduction to millimeter-wave mobile broadband systems. *IEEE Commun. Mag.* **2011**, *49*, 101–107. [[CrossRef](#)]
7. Nadeem, I.; Choi, D.-Y. Study on Mutual Coupling Reduction Technique for MIMO Antennas. *IEEE Access* **2018**, *7*, 563–586. [[CrossRef](#)]
8. Kumar, S.; Dixit, A.S.; Malekar, R.R.; Raut, H.D.; Shevada, L.K. Fifth Generation Antennas: A Comprehensive Review of Design and Performance Enhancement Techniques. *IEEE Access* **2020**, *8*, 163568–163593. [[CrossRef](#)]
9. Dixit, A.S.; Kumar, S. A Survey of Performance Enhancement Techniques of Antipodal Vivaldi Antenna. *IEEE Access* **2020**, *8*, 45774–45796. [[CrossRef](#)]
10. Farida, S.F.; Hadalgi, P.; Hunagund, P.; Ara, S.R. Effect of substrate thickness and permittivity on the characteristics of rectangular microstrip antenna. In Proceedings of the 1998 Conference on Precision Electromagnetic Measurements Digest (Cat. No. 98CH36254), Washington, DC, USA, 6–10 July 1998. [[CrossRef](#)]
11. Honari, M.M.; Ghaffarian, M.S.; Mousavi, P.; Sarabandi, K. A Wideband High-Gain Planar Corrugated Antenna. In Proceedings of the 2020 IEEE International Symposium on Antennas and Propagation and North American Radio Science Meeting, Montreal, QC, Canada, 5–10 July 2020; pp. 7–8. [[CrossRef](#)]
12. Wang, Z.; Dou, W. Dielectric lens antennas designed for millimeter wave application. In Proceedings of the 2006 Joint 31st International Conference on Infrared Millimeter Waves and 14th International Conference on Terahertz Electronics, Shanghai, China, 18–22 September 2006; p. 376. [[CrossRef](#)]
13. Zhang, Z.; Li, X.; Sun, C.; Liu, Y.; Han, G. Dual-Band Focused Transmitarray Antenna for Microwave Measurements. *IEEE Access* **2020**, *8*, 100337–100345. [[CrossRef](#)]
14. Dey, S.; Dey, S.; Koul, S.K. Isolation Improvement of MIMO Antenna Using Novel EBG and Hair-Pin Shaped DGS at 5G Millimeter Wave Band. *IEEE Access* **2021**, *9*, 162820–162834. [[CrossRef](#)]

15. Goswami, C.; Roy, B.; Bhattacharya, P.; Ray, S.; Ghosh, S.; Ghosh, D.; Saha, D.; Jana, T.; Chatterjee, S. Complementary Split Rings Resonator Based Circular Microstrip Antenna for Wireless Applications. In Proceedings of the 2019 IEEE International Electromagnetics and Antenna Conference (IEMANTENNA), Vancouver, BC, Canada, 17–19 October 2019; pp. 065–067. [CrossRef]
16. Ziolkowski, R.W. Metamaterials and Antennas. In *Handbook of Antenna Technologies*; Chen, Z., Liu, D., Nakano, H., Qing, X., Zwick, T., Eds.; Springer: Singapore. [CrossRef]
17. Chen, Z.; Tang, M.-C.; Wang, Y.; Li, M.; Li, D. Mutual Coupling Reduction Using Planar Parasitic Resonators for Wideband, Dual-Polarized, High-Density Patch Arrays. In Proceedings of the 2019 IEEE MTT-S International Wireless Symposium (IWS), Guangzhou, China, 19–22 May 2019; pp. 1–3. [CrossRef]
18. Iqbal, A.; Saraereh, O.A.; Ahmad, A.W.; Bashir, S. Mutual Coupling Reduction Using F-Shaped Stubs in UWB-MIMO Antenna. *IEEE Access* **2017**, *6*, 2755–2759. [CrossRef]
19. Chandel, R.; Gautam, A.K.; Rambabu, K. Tapered Fed Compact UWB MIMO-Diversity Antenna with Dual Band-Notched Characteristics. *IEEE Trans. Antennas Propag.* **2018**, *66*, 1677–1684. [CrossRef]
20. Karaboikis; Soras; Tsachtsiris; Makios Compact dual-printed inverted-F antenna diversity systems for portable wireless devices. *IEEE Antennas Wirel. Propag. Lett.* **2004**, *3*, 9–14. [CrossRef]
21. Li, Z.; Yin, C.; Zhu, X. Compact UWB MIMO Vivaldi Antenna With Dual Band-Notched Characteristics. *IEEE Access* **2019**, *7*, 38696–38701. [CrossRef]
22. El-Din, M.S.H.S.; Shams, S.I.; Allam, A.M.M.A.; Gaafar, A.; Elhennawy, H.M.; Sree, M.F.A. SIGW Based MIMO Antenna for Satellite Down-Link Applications. *IEEE Access* **2022**, *10*, 35965–35976. [CrossRef]
23. Alibakhshikenari, M.; Virdee, B.S.; See, C.H.; Abd-Alhameed, R.; Falcone, F.; Limiti, E. A new waveguide slot array antenna with high isolation and high antenna bandwidth operation on Ku- and K-bands for radar and MIMO systems. In Proceedings of the 2018 15th European Radar Conference (EuRAD), Madrid, Spain, 26–28 September 2018; pp. 401–404.
24. Alibakhshikenari, M.; Virdee, B.S.; See, I.C.H.; Abd-Alhameed, R.; Falcone, F.; Andújar, A.; Anguera, J.; Limiti, E. Study on antenna mutual coupling suppression using integrated metasurface isolator for SAR and MIMO applications. In Proceedings of the 2018 48th European Microwave Conference (EuMC), Madrid, Spain, 23–27 September 2018; pp. 1425–1428.
25. Biswas, A.K.; Chakraborty, U. Textile Multiple Input Multiple Output Antenna for X-Band and Ku-Band Uplink-downlink Applications. In Proceedings of the 2020 National Conference on Emerging Trends on Sustainable Technology and Engineering Applications (NCETSTEA), Durgapur, India, 7–8 February 2020; pp. 1–4. [CrossRef]
26. Kumar, N.; Kumar, P.; Sharma, M. Superwideband Dual Notched Band Square Monopole MIMO Antenna for UWB/X/Ku Band Wireless Applications. In Proceedings of the 2019 IEEE Indian Conference on Antennas and Propagation (InCAP), Ahmedabad, India, 19–22 December 2019; pp. 1–5. [CrossRef]
27. Sharawi, M.S. Printed Multi-Band MIMO Antenna Systems and Their Performance Metrics [Wireless Corner]. *IEEE Antennas Propag. Mag.* **2013**, *55*, 218–232. [CrossRef]
28. Sharawi, M.S. *Printed MIMO Antenna Engineering*; Artech House: Norwood, MA, USA, 2014.
29. Manteghi, M.; Sami, Y.R. Broadband Characterization of the Total Active Reflection Coefficient of Multiport Antennas. In Proceedings of the IEEE Antennas and Propagation Society International Symposium (APS2003), Columbus, OH, USA, 22–27 June 2003; Volume 3, pp. 20–23.
30. Abdelraheem, A.; Elregaily, H.; Mitkees, A.A.; Abdalla, M. A Hybrid Isolation in Two-Element Directive UWB MIMO Antenna. *IETE J. Res.* **2020**, *69*, 499–508. [CrossRef]
31. Available online: <https://rogerscorp.com/advanced-electronics-solutions/ro4000-series-laminates/ro4003c-laminates>. (accessed on 20 December 2021).
32. Available online: <https://rogerscorp.com/-/media/project/rogerscorp/documents/advanced-electronics-solutions/english/data-sheets/ro4000-laminates-ro4003c-and-ro4350b---data-sheet.pdf>. (accessed on 20 December 2021).
33. Available online: https://scdn.rohde-schwarz.com/ur/pws/dl_downloads/dl_common_library/dl_brochures_and_datasheets/pdf_1/ZVA_dat-sw_en_5213-5680-22_v1400.pdf. (accessed on 20 December 2021).
34. Balanis, C. *Antenna Theory: Analysis and Design*; Wiley: New York, NY, USA, 1997.
35. Sarkar, D.; Mikki, S.; Srivastava, K.V.; Antar, Y. Far-field Envelope Correlation Coefficient and Near-field Reactive Energy of MIMO Antennas: An FDTD-IDM-CGF Approach. In Proceedings of the 2019 URSI Asia-Pacific Radio Science Conference (AP-RASC), New Delhi, India, 9–15 March 2019. [CrossRef]
36. Mei, X.; Wu, K.-L. Envelope Correlation Coefficient for Multiple MIMO Antennas of Mobile Terminals. In Proceedings of the 2020 IEEE International Symposium on Antennas and Propagation and North American Radio Science Meeting, Montreal, QC, Canada, 5–10 July 2020; pp. 1597–1598. [CrossRef]
37. Tariq, S.; Naqvi, S.I.; Hussain, N.; Amin, Y. A Metasurface-Based MIMO Antenna for 5G Millimeter-Wave Applications. *IEEE Access* **2021**, *9*, 51805–51817. [CrossRef]
38. Tian, R.; Lau, B.K.; Ying, Z. Multiplexing Efficiency of MIMO Antennas. *IEEE Antennas Wirel. Propag. Lett.* **2011**, *10*, 183–186. [CrossRef]
39. Chae, S.H.; Kawk, W.I.; Park, S.-O.; Lee, K. Analysis of mutual coupling in MIMO antenna array by TARC calculation. In Proceedings of the 2006 Asia-Pacific Microwave Conference, Yokohama, Japan, 12–15 December 2006; pp. 2090–2093. [CrossRef]
40. Wu, A.; Zhao, M.; Zhang, P.; Zhang, Z. A Compact Four-Port MIMO Antenna for UWB Applications. *Sensors* **2022**, *22*, 5788. [CrossRef]

41. Bilal, M.; Naqvi, S.I.; Hussain, N.; Amin, Y.; Kim, N. High-Isolation MIMO Antenna for 5G Millimeter-Wave Communication Systems. *Electronics* **2022**, *11*, 962. [[CrossRef](#)]
42. Fat, S.Y.A.; Hamad, E.K.I.; Swelam, W.; Allam, A.M.; Mohamed, H.A.E. Design of compact 4-port MIMO antenna based on Minkowski fractal shape DGS for 5G applications. *Prog. Electromagn. Res. C* **2021**, *113*, 123–136. [[CrossRef](#)]
43. Kumar, A. Compact 4×4 CPW-Fed MIMO Antenna with Wi-Fi and WLAN Notch for UWB Applications. *Radioelectron. Commun. Syst.* **2021**, *64*, 92–98. [[CrossRef](#)]
44. Hussain, M.; Ali, E.M.; Jarchavi, S.M.R.; Zaidi, A.; Najam, A.I.; Alotaibi, A.A.; Althobaiti, A.; Ghoneim, S.S.M. Design and Characterization of Compact Broadband Antenna and Its MIMO Configuration for 28 GHz 5G Applications. *Electronics* **2022**, *11*, 523. [[CrossRef](#)]
45. Li, M.-Y.; Ban, Y.-L.; Xu, Z.-Q.; Guo, J.; Yu, Z.-F. Tri-Polarized 12-Antenna MIMO Array for Future 5G Smartphone Applications. *IEEE Access* **2017**, *6*, 6160–6170. [[CrossRef](#)]
46. Fatah, S.Y.A.; Hamad, E.K.I.K.I.; Swelam, W.; Allam, A.M.M.A.; Sree, M.F.A.; Mohamed, H.A. Design and Implementation of UWB Slot-Loaded Printed Antenna for Microwave and Millimeter Wave Applications. *IEEE Access* **2021**, *9*, 29555–29564. [[CrossRef](#)]

Disclaimer/Publisher’s Note: The statements, opinions and data contained in all publications are solely those of the individual author(s) and contributor(s) and not of MDPI and/or the editor(s). MDPI and/or the editor(s) disclaim responsibility for any injury to people or property resulting from any ideas, methods, instructions or products referred to in the content.